Journal of Power Sources 429 (2019) 111–119

Contents lists available at ScienceDirect

Journal of Power Sources

journal homepage: www.elsevier.com/locate/jpowsour

Development of a facile and low-cost chitosan-modified carbon cloth for efficient self-pumping enzymatic biofuel cells

Ngoc Bich Duong [a], Chih-Liang Wang [a,*], Li Zhen Huang [a], Wan Ting Fang [a], Hsiharng Yang [a,b,**]

[a] Graduate Institute of Precision Engineering, National Chung Hsing University, 145 Xingda Road, South District, Taichung City, 402, Taiwan
[b] Innovation and Development Center of Sustainable Agriculture (IDCSA), National Chung Hsing University, 145 Xingda Road, South District, Taichung City 402, Taiwan

ARTICLE INFO

Keywords:
Enzymatic biofuel cell
Self-pumping EBC
Immobilized enzyme
Chitosan-modified carbon cloth

ABSTRACT

Enzymatic biofuel cell (EBC) attracts much attention recently in fuel cell community because of its unique feature to enable the enzyme as a catalyst, rather than precious metal, to oxidize the fuel. However, the embedment of carbon nanotubes, commonly used in the anodic electrode of EBC to electrically wire the enzyme, suffers from their complicated synthetic procedure and fragile assembly. In this regard, we demonstrate a facile and low-cost route to achieve a desired immobilization of the glucose oxidase on a robust, flexible conducive carbon cloth. Our result indicates that the EBC using chitosan-modified carbon cloth via tripolyphosphate as anodic electrode exhibits a better performance than that via Nafion, leading to a 53% improvement of area power density. Such an enhancement can be attributed to the formation of the open porous structure on chitosan-modified carbon cloth, beneficial for the immobilization sites of the glucose oxidase and thereby facilitating more electron transfer in glucose oxidation reaction. The self-pumping EBC, driven by a capillary force of micro-fluidic channel plate, delivers an efficient area and volume power density of 0.549 $mWcm^{-2}$ and 114.52 $mWcm^{-3}$, respectively, enabling to open an alternative to the lightweight and portable applications.

1. Introduction

Sustainable energy and alternative fuel sources such as solar energy, hydrogen, biomass and biofuels have been exploited by many scientists and researchers. Among utilization of these energy sources, a biofuel cell that directly converts chemical energy into electricity via living biocatalysts [1,2] is one of the most promising topics because of its environmentally friendly characteristics as a renewable energy. The biofuel cell can be categorized into microbial biofuel cell (MBC) and enzymatic biofuel cell (EBC) [3,4]. Although the MBC and EBC both utilize the chemical energy of organics to produce the electricity, the enzyme-involved EBC showing the higher electrochemical performance and simple structure is increasingly appealing to fuel cell community [5,6]. The working principle of EBC is given as follows.

Anode:

$$C_6H_{12}O_6 + H_2O \xrightarrow{GOx} C_6H_{12}O_7 + 2e^- + 2H^+$$

Cathode:

$$2Fe(CN)_6^{3-} + 2e^- \rightarrow 2Fe(CN)_6^{4-}$$

$$2Fe(CN)_6^{4-} + 2H^+ + \frac{1}{2}O_2 \rightarrow 2Fe(CN)_6^{3-} + H_2O$$

Total:

$$C_6H_{12}O_6 + \frac{1}{2}O_2 \rightarrow C_6H_{12}O_7$$

One of the enzymes, commonly used in biofuel cell, is glucose oxidase (GOx) immobilized as a catalyst at the anode to oxidize glucose into gluconolactone [7,8] while its released electrons and protons make the reduction of oxygen to produce the water at the cathode [9]. Accordingly, it can be known that the immobilization of enzyme plays a critical role in the operation of EBC. A variety of methods based on physical and chemical routes have been developed for the enzyme immobilization [10]. The commonly used methods of the enzymes immobilized on the electrode are the adsorption [11,12], the entrapment in conducting polymer matrices [13–15], covalent attachment to functionalized polymers [16,17], and crosslinking [18]. It can be found that the

* Corresponding author.
** Corresponding author. Graduate Institute of Precision Engineering, National Chung Hsing University, 145 Xingda Road, South District, Taichung City, 402, Taiwan.
E-mail addresses: clwang@email.nchu.edu.tw (C.-L. Wang), hsiharng@dragon.nchu.edu.tw (H. Yang).

https://doi.org/10.1016/j.jpowsour.2019.05.001
Received 29 January 2019; Received in revised form 19 April 2019; Accepted 1 May 2019

biocatalystic ability strongly depends on the interplay of the enzyme and the underlying support material during the immobilization. However, the selection of the support material is the most challenging due to its impact on the properties of the biocatalytic system [19]. Among all the support materials, chitosan (CS) is particularly considered as a promising material for GOx immobilization due to its inherent properties such as biocompatibility, biodegradability, chemical inertness, low toxicity, and abundance [20]. Accordingly, research studies of combining CS with GOx have been reported. For example, H. Susanto et al. [21] demonstrated a concept of the immobilization of GOx onto porous CS-based composite membranes with and without glutaraldehyde (GA) in a biosensor. S. El Ichi et al. [22] proposed a combined bio-cathode of using CS, carbon nanotube (CNT) and enzyme to allowedly improve not only the long-term stability of the current density but also the biocompatibility for use in implantable biofuel cells. S.W. Buckner et al. [23] prepared a metallacarborane redox mediator for an enzyme-immobilized CS-modified bioanode. Y. Huang et al. [24] prepared an outer-layer CS film to prevent the enzyme leaching and mechanically strengthen the enzyme film by casting CS solution on the enzyme electrode of GOx-PABA-Au_{nano}/Au-plated Au in biosensor and biofuel cell. From these studies, it can be known that the electrode embedded with carbon nanotubes shows a useful, cost-effective way to provide the advantages of electroactive surface, porosity and electron transfer for the immobilized enzyme and fast reaction. However, the device performance of EBC strongly relies on the interconnected carbon nanotubes within the ensemble electrode. While T. Miyake et al. [25] prepared an efficient carbon nanotube-enzyme disk electrodes by mechanical compression, A. Zebda et al. [26] also fabricated a self-regulating enzyme-nanotube ensemble films by the chemical vapor deposition. Unfortunately, the above-mentioned approaches remain challenging and complex to completely avoid the aggregates of carbon nanotubes, limiting the feasibility of reproducibly reaching a scalable and high-performance electrode. Different from easily fractured nature of interconnected carbon nanotube electrode, carbon cloth (CC) based electrode can provide a robust and excellent conductive substrate for the immobilized enzymes and the electron transfer. Accordingly, we proposed a facile and low-cost route to achieve a desired immobilization of the GOx on the CS-modified conducive CC.

The CS is polycationic in acidic media and can interact with negatively charged species such as tripolyphosphate (TPP) and sodium sulfate to form the cross-linked TPP/CS composites. D. R. Bhumkar et al. [27] further studied the effect of pH values on cross-linking of CS with TPP. The ionic interaction of cross-linked TPP/CS between the positively charged CS and negatively charged phosphoric ions is found to have the tendency to form at lower pH condition, being suitable for the biosensors [28–30] and biomedical applications [27,31–34]. M. M. Hasani-Sadrabadi et al. [35] also showed that the incorporation of CS-coated carbon nanotubes into a Nafion matrix results in the improvement of the proton conductivity and membrane selectivity for direct methanol fuel cell (DMFC). Previous studies show that the CS combined with certain species or additives can provide the optimization for the immobilized enzymes in different applications. Unfortunately, the study of the effect of extra additive on CS-modified CC for the immobilized enzyme in EBC seemingly remains few.

On the other hand, the operation of EBC, typically required with an external pump to render the delivery of the fuel, recently comes to the scientific notice because of the power consumption of the external pump potentially overweighting the output power of the fuel cell. In addition, the EBC driven by an external pump is facing the challenge in the miniaturization and thereby compromises on its lightweight and portable applications such as implantable battery-powered and microscale devices [30,36–38]. To circumvent such the problems, some researchers have worked on the development of a self-driven actuation motion via the capillary effect during the operation of fuel cells [39–41]. However, most of the studies on the self-driven flow fuel cell had previously been focused on DMFC, rather than EBC. As a result, the development of self-pumping EBC driven by the capillary effect is urgently required to understand its device performance and evaluate the possibility of lightweight and portable applications.

These above-mentioned requirements motivate us to explore the development of a facile and low-cost route to effectively immobilize the GOx on conducive CC for use in self-pumping EBC. The TPP and Nafion ($Na^{®}$) are chosen as the additive in this study because of their advantages of low toxicity, low cost, and ecological benefits [32,33,42]. The different CS-modified CCs are prepared by adding TPP and $Na^{®}$ into the CS-modified CCs and named as TPP/CS/CC and $Na^{®}$/CS/CC, respectively. The precipitation of the enzyme on TPP/CS/CC and $Na^{®}$/CS/CC to form GOx [TPP/CS/CC] and GOx [$Na^{®}$/CS/CC], respectively, are subsequently prepared to investigate the role of the additives on the immobilized enzyme of CS-modified CC as the anodic electrode of EBC. Our result shows that the EBC using anodic electrode of GOx [TPP/CS/CC] exhibits a better performance than that of GOx [$Na^{®}$/CS/CC], leading to a 53% improvement of area power density. Such an enhancement can be attributed to the improved immobilization of the enzyme on CS-modified carbon cloth by the additive. When miniaturizing from the typical EBC to the self-pumping EBC (without external pump), its device performance of using anodic electrode of GOx [TPP/CS/CC] is obtained with volume power density of 114.52 $mWcm^{-3}$, higher than that of 14.71 $mWcm^{-3}$ (typical EBC), demonstrating the potential and possibility of a self-driven actuation motion via the capillary effect during the operation of EBC.

2. Experimental

2.1. Materials

Carbon cloth (CC) was obtained from CeTech Co. (Taichung, Taiwan). Glucose oxidase (GOx) from Aspergillus Niger (Gluzyme Mono® 10000 BG) was purchased from Novo Nordisk Bio Industrials Inc. (Copenhagen, Denmark). The chitosan (CS) powder (MW 140000 dal/mol) with 90% deacetylation and sieved using a 100-mesh filter was purchased from Shin ERA Tech. Co. Ltd. (Taipei, Taiwan). Sodium tripolyphosphate (TPP), potassium hexacyanoferrate III (K_3 [$Fe(CN)_6$], 1-ethyl-3-(3-dimethylaminopropyl)carbodiimide (EDC) were purchased from Sigma-Aldrich (MO, USA). N-hydroxysuccinimide (NHS) was purchased from Alfar Aesar (Massachusetts, USA). Nafion perflourinated resin solution ($Na^{®}$ solution), 5 wt% in mixture of lower aliphatic alcohols and water, containing 45% water was purchased from Sigma-Aldrich. Nafion®117 membranes (DuPont) were activated by using the heated hydrogen peroxide and sulfuric acid baths before use.

2.2. Preparation of anodic electrode

2.2.1. Chitosan-modified carbon cloth

The chitosan (CS) solution was firstly prepared by dissolving 2 g of CS powders in 200 mL of 2% (v/v) acetic acid. To prepare a mixed solution of TPP and CS, 100 mL of CS solution was then added with 25 mL of TPP solution (1 mg mL^{-1}) as a cross-linker. To prepare a mixed solution of $Na^{®}$ and CS, 100 mL of CS solution was added with 3 mL of $Na^{®}$ solution. Both of the mixed solutions were stirred at room temperature for 10 min. The CC was treated to become hydrophilic CC by immersing in the mixed acid solution of H_2SO_4:HNO_3 (3:1) for 20 min, followed by deionized water washing for several times to remove extra acid solution before use. The samples of TPP/CS-coated and $Na^{®}$/CS-coated CC were prepared by the immersion of as-treated CCs ($8.2 \times 8.2\ cm^2$) in each of the above-mentioned mixed solutions under a sonication bath for 30 min and then into 1 M NaOH aqueous solution for the precipitation of CS on top of CC. Afterwards, these samples were followed by the washing procedure (3 h) using deionized water three times to remove the residue of NaOH solution.

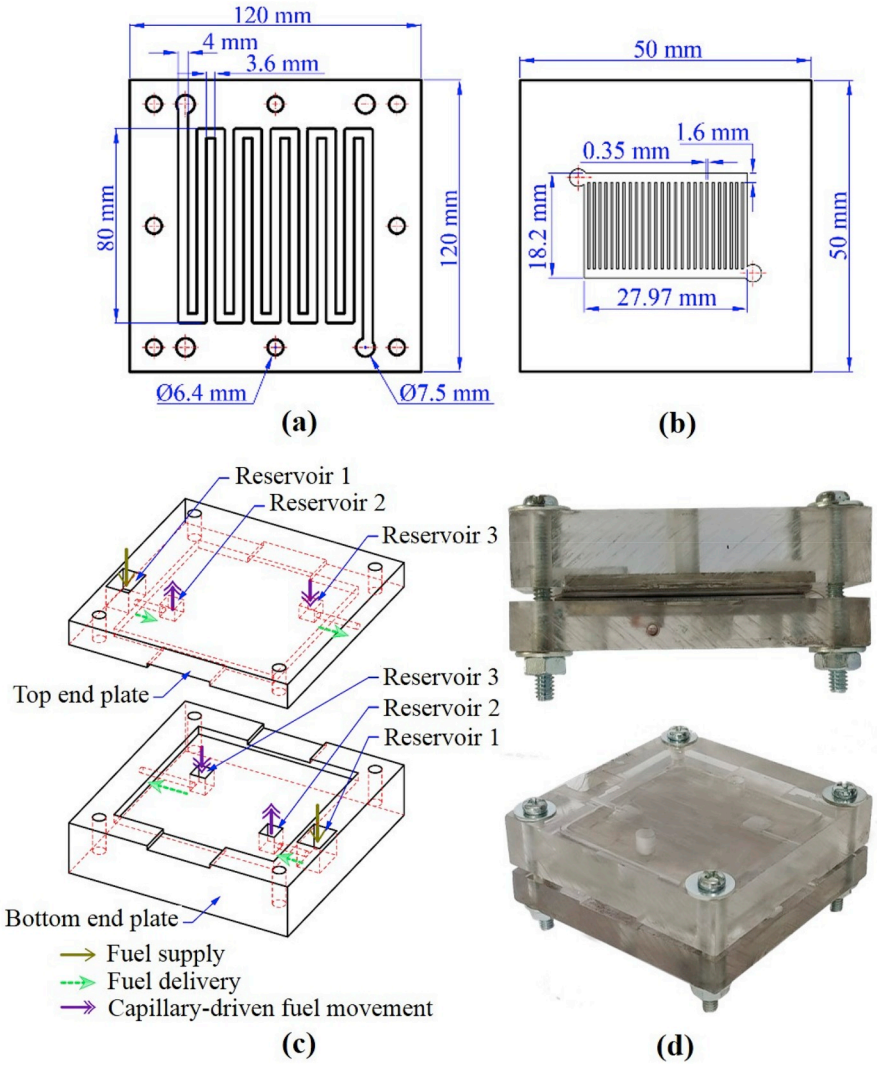

Fig. 1. The design of flow channel plates for (a) typical EBC (with pump) and (b) self-pumping EBC (without pump); (c) schematic diagram of top and bottom end plates in the self-pumping EBC stack and (d) photograph of self-pumping EBC assembly.

2.2.2. *Immobilization of glucose oxidase onto chitosan-modified carbon cloth*

The solution of GOx was prepared by adding 3.42 g of GOx dissolved into 200 mL of phosphate buffered saline (PBS, pH = 6) with 324 mg of EDC, following by shaking for 1 h at 120 rpm for enzyme activation. The carboxyl group of the enzyme, coupled with the primary amine of EDC, can help become an active ester. To increase the stability of the active ester and prevent the reduction of enzyme, 194.4 mg of NHS was added to the solution of GOx under the magnetic stirrer at 120 rpm for 1 h. The samples of GOx immobilized onto different CS-modified CCs, GOx [TPP/CS/CC] and GOx [Na®/CS/CC], as anodic electrodes can be obtained by rinsing and shaking TPP/CS-coated and Na®/CS-coated CC, respectively, into the solution of activated GOx for 1 h. Afterwards, another washing procedure using deionized water was conducted to remove the excess reagent or unwanted by-products and then stored in deionized water until use.

2.3. *Characterization*

Field emission scanning electron microscopy (FE-SEM) (JEOL, JSM-7600F) was performed to characterize the surface morphology of anodic electrodes. Attenuated total reflection Fourier transform infrared (ATR-FTIR) spectroscopy (Bruker Vertex 70 V, Hyperion 3000) was used to analyze the chemical structure of different anodic electrodes. Cyclic voltammetry (CV) (Zahner, Zennium E Electrochemical Workstation) was carried out to understand the electron transfer ability of different anodic electrodes. The CV test was performed using a 3-electrode system with the reference electrode (Ag/AgCl), counter electrode (Pt wire) and working electrode. The working electrodes of GOx/TPP/CS and GOx/Na®/CS were prepared on glassy carbon electrode (GCE). All the CV analyses were tested at scan rate of 100 mV s^{-1} in the potential range from −1.0 to 1.0 V with glucose-free (PBS, pH = 7.0) or the mixed solution of 0.1 M glucose and 0.1 M NaCl electrolyte. The performance test was conducted by a microfuel cell test station (EL505R3, Beam Associate Co. Ltd., Taiwan).

2.4. *Assembly of EBC*

The stack configuration of self-pumping EBC consists of the top and bottom end plates, two copper current collectors, two flow channel plates, and two Polydimethyl Siloxane (PDMS) gaskets. The activated Nafion®117 (proton exchange membrane) was sandwiched by the anodic electrode (different CS-modified CCs as described in section 2.2) and cathodic electrode (unmodified CC) without the hot pressing. The active area of the electrodes utilized in the self-pumping EBC and the typical EBC were 3.86 cm^2 and 33.8 cm^2, respectively. The membrane electrode assembly (MEA) was secured by two stainless steels with flow channels, as described in section 2.5, and copper current collector

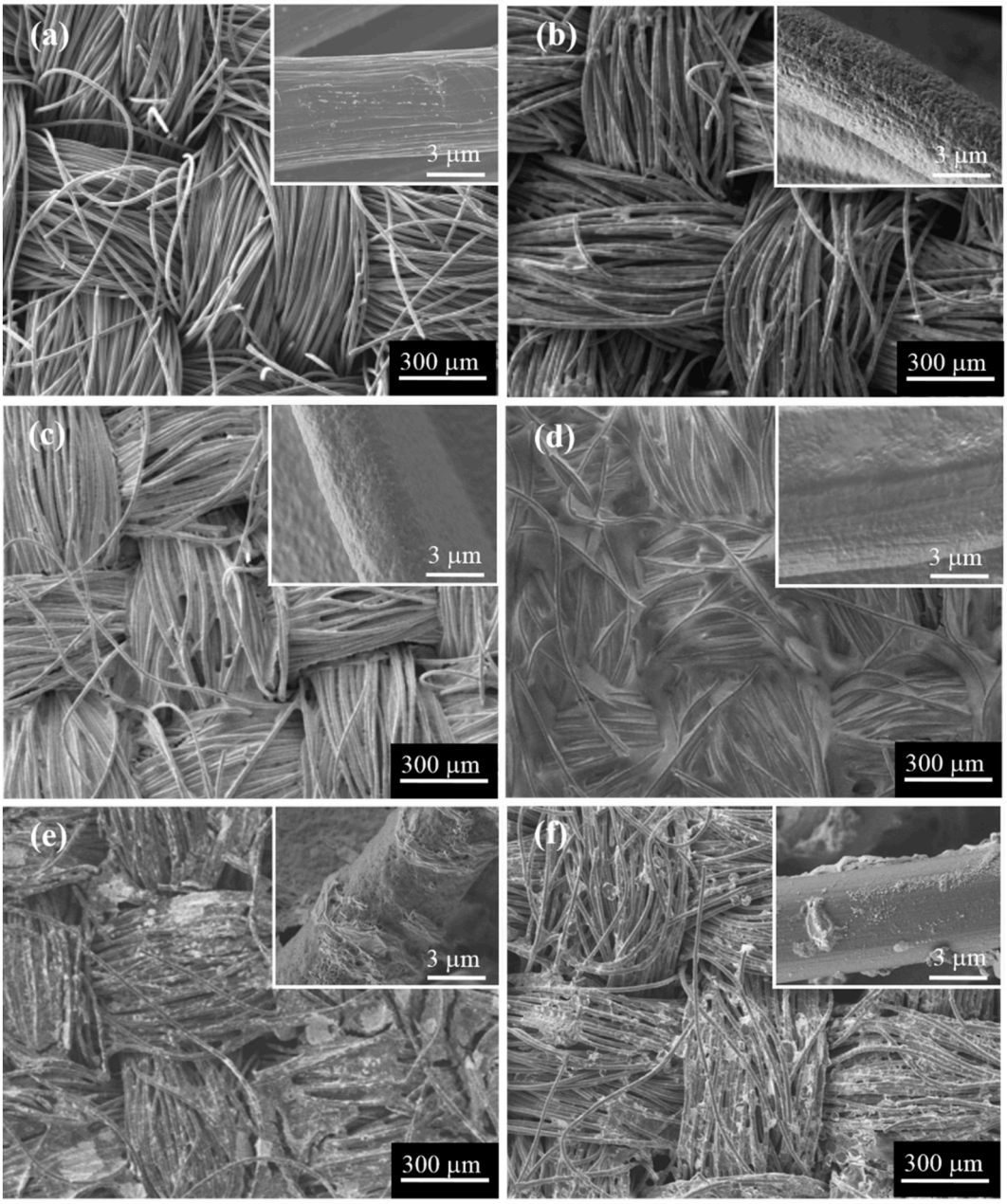

Fig. 2. Low-magnification and high-magnification (inset) SEM images of (a) CC, (b) CS/CC, (c) TPP/CS/CC, (d) Na®/CS/CC, (e) GOx [TPP/CS/CC] and (f) GOx [Na®/CS/CC].

plates. During the testing, the mixture of 0.1 M glucose solution and 0.1 M NaCl solution (PBS, pH = 7) was fed at the anode side while 0.1 M $K_3Fe(CN)_6$ solution was fed at the cathode side. For the stability evaluation, the performance of self-pumping EBC was measured at 24 h, 72 h, 120 h and 240 h at room temperature. All these serial measurements were conducted without replacing the new membrane in-between. The cell right after each testing was stored in a refrigerator at −4 °C, as suggested by the enzyme manufacturer, to prevent the degradation of GOx from ambient temperature.

2.5. Design of self-pumping EBC

The typical EBC and self-pumping EBC rely on the same electrochemical mechanism to convert the fuel into the electricity. However, the different concept of fuel supply between the typical EBC and self-pumping EBC makes the design of flow channel plate distinct, as shown in Fig. 1(a) and Fig. 1(b). The flow plate of parallel type pattern composed of 27 channels for self-pumping EBC is detailed as shown in Table S1. It can be found that the fuel supply of self-pumping EBC based on the capillary effect is allowed to miniaturize its dimension of flow channel plate and thereby provide the advantages of the lightweight and portable applications. In addition, there are extra three reservoirs designed on top and bottom end plates of self-pumping EBC stack, as shown in Fig. 1(c). The photograph of self-pumping EBC assembly is shown in Fig. 1(d). The function of reservoir 1 is the fuel supply while that of reservoirs 2 and 3 loaded with cottons can be offered with a self-driven source to create the capillary effect. During the operation, the fuel is firstly added into the reservoir 1, transported to reservoir 2 by capillary force, and arrived at the inlet of flow channel plate. The fuel then flows through the anode/cathode flow channel plate where the oxidation/reduction reaction occurs. Once the fuel reaches the outlet of flow channel plate, the wetted cotton in reservoir 3 can be observed. The

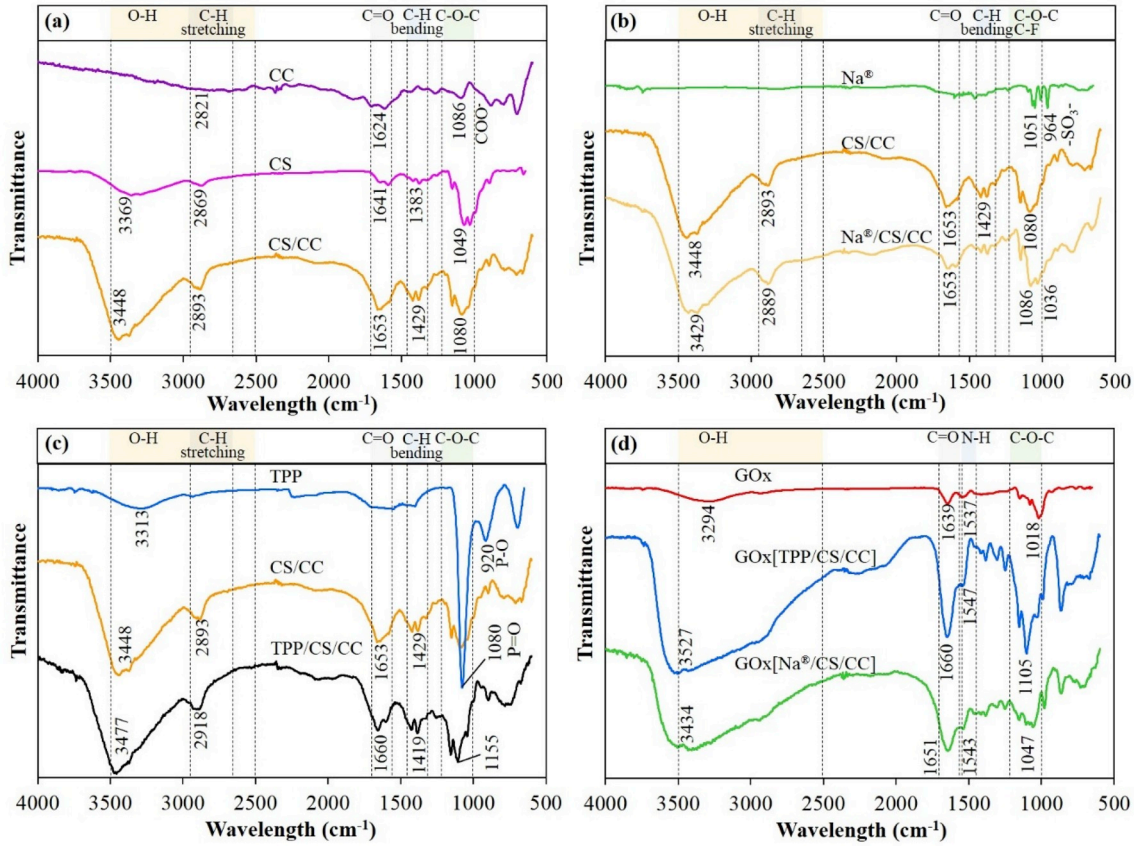

Fig. 3. FTIR spectra of (a) CC, CS, and CS/CC, (b) Na®, CS/CC, Na®/CS/CC, (c) TPP, CS/CC, TPP/CS/CC, and (d) GOx, GOx [TPP/CS/CC], GOx [Na®/CS/CC].

flow rate can be determined by collecting 500 mm^3 each time of fuel and recording the elapsed time. The flow channel plate of self-pumping EBC can be fabricated by using a lithographic process, as mentioned in the reference [43]. To improve the hydrophilic ability of the flow channel plate, the as-prepared plates were firstly immersed in 1.5 wt% poly (diallyl dimethyl ammonium chloride) (PDDA) and then dispersed with 0.5 M NaCl for 15 min at room temperature. The plates were finally rinsed with deionized water, followed by dipping into 0.3 wt% poly (styrenesulfonate) (PSS) with 0.5 M NaCl for 15 min.

3. Results and discussion

3.1. The microstructure of various anodic electrodes

The surface morphology of different anodic electrodes was carried out by FE-SEM. The samples of pristine CC, CS-modified CC (CS/CC), TPP/CS-modified CC (TPP/CS/CC), Na®/CS-modified CC (Na®/CS/CC), the immobilization of GOx on TPP/CS-modified CC (GOx [TPP/CS/CC]), and the immobilization of GOx on Na®/CS-modified CC (GOx [Na®/CS/CC]) were prepared, as shown in Fig. 2, to investigate the surface morphology of anodic electrodes varied with the different additives. Our result of Fig. 2(a) indicates that the pristine CC is assembled with the intercrossed fibers with an average diameter of 5.5 μm. After the immersion of pristine CC into the CS solution, the smooth surface of the fibers in the pristine CC is found to become a porous morphology, as shown in the inset of Fig. 2(b), suggesting the formation of CS is unevenly deposited on the surface of the fibers.

On the other hand, the samples of TPP/CS-modified CC and Na®/CS-modified CC, as shown in Fig. 2(c) and (d), are both presented a smooth surface of the fibers fully covered with CS, confirming the addition of TPP or Na® into the CS solution is beneficial for the uniformly distribution of CS on CC. However, from the inset of Fig. 2(c) and (d), TPP/CS-modified CC still shows a relatively open porous structure than Na®/CS-modified CC, suggesting the different formation processes of CS-modified CC between the cross-linked TPP/CS nanoparticles and polymeric matrix of Na®/CS composite [35,44–46]. Such a porous nanoscale structure, as shown in Fig. S1, could be beneficial for the biocatalyst due to the improvement of specific surface area, mass transfer resistance, and enzyme loading [47,48]. The morphology of immobilized enzymes on TPP/CS-modified CC and Na®/CS-modified CC are shown in Fig. 2(e) and (f), respectively. It can be found that the amount of GOx distributed on TPP/CS-modified CC is higher than that on Na®/CS-modified CC while the porous surface morphology of TPP/CS-modified CC after the immobilized enzyme process (the inset of Fig. 2(e)) remains the same as that before (the inset of Fig. 2(c)). In contrast, the porous surface morphology of Na®/CS-modified CC after the immobilized enzyme process (the inset of Fig. 2(f)) almost disappears. Such a result indicates that the additive of TPP can function not only as a robust adhesion to form CS-modified CC but also a cross-linker to form a suitable porous structure with the immobilization of the enzymes.

3.2. The chemical structure of various anodic electrodes

The FTIR spectra of CS, CC, and CS/CC, recorded from 500 to 4000 cm^{-1}, are presented in Fig. 3(a) to systemically analyze the chemical structure of different anodic electrodes. The FTIR spectrum of CC shows the presence of carboxyl functional groups C═O stretching vibration at 1624 cm^{-1}, COO^- at 1086 cm^{-1}, and its broad peak of 2821 cm^{-1} assigned to the group of O-H (carboxylic acid), indicating that the carboxyl group has been successfully attached onto the surface of CC as well as the hydrophilic characteristic of CC [49,50].

It can be observed that the CS shows the three main FTIR peaks of O-H band at 3369 cm^{-1}, C═O stretching bond at 1641 cm^{-1}, and C-O-C asymmetric stretching at 1049 cm^{-1} [34]. The FTIR spectrum of CC after

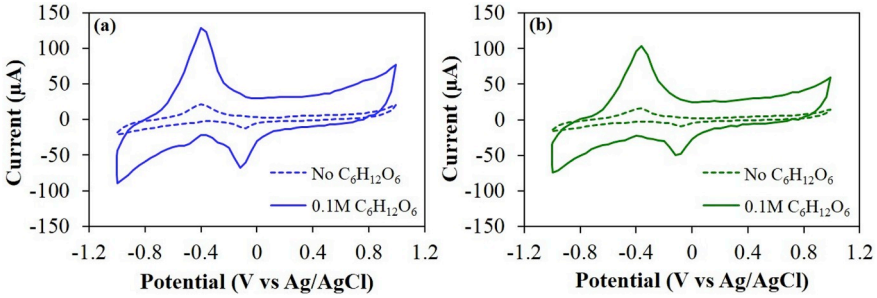

Fig. 4. CV of (a) GOx/TPP/CS and (b) GOx/Na®/CS on GCE in phosphate buffer saline (PBS, pH = 7) with and without 0.1 M $C_6H_{12}O_6$ at 100 mVs^{-1}.

coating CS shows the stretching vibrations of O-H at 3448 cm^{-1}, C-H stretching at 2893 cm^{-1}, the glycosidic linkage of C-O-C bridge stretching at 1080 cm^{-1}, C-H bending group at 1429 cm^{-1}, and the acetamide group (Amide I) of C═O at 1653 cm^{-1}. Such a result indicates that CS via our approach can be successfully coated on CC, as consistent with the result of Fig. 2(b).

The chemical structure of CS/CC with the addition of Na® was investigated as shown in Fig. 3(b). The FTIR spectrum of Na® solution shows two main weak peaks of C-F stretching vibrations at 1051 cm^{-1} and SO_3^- symmetric stretching vibrations at 964 cm^{-1} [51–53]. As compared to the FTIR spectrum of CS/CC, the sample of Na®/CS/CC shows the extra peaks of C-F (1036 cm^{-1}) from Na® and the shift of the peaks, suggesting the addition of Na® is involved into CS-modified CC.

On the other hand, the FTIR spectrum of TPP, as shown in Fig. 3(c), indicates the two main peaks of asymmetric P═O stretching at 1080 cm^{-1} and P-O stretch symmetric at 920 cm^{-1} [34]. When comparing TPP/CS/CC with CS/CC, the shift of the peaks can be observed as well. The peak position of C═O stretching vibration at 1653 cm^{-1} and O-H broad band at 3448 cm^{-1} in CS/CC are shifted to 1660 cm^{-1} and 3477 cm^{-1}, respectively, in TPP/CS/CC due to the cross-link of TPP and CS [27,54,55]. The asymmetric stretching vibration of PO_2^- groups at 1080 cm^{-1} confirms the formation of ionic cross-link between NH_3^+ groups of CS and TPP ions [56]. When linking the SEM results of CS/CC, Na®/CS/CC or TPP/CS/CC to the FTIR results, it can be known that the additive of Na® or TPP in CS/CC can be beneficial for the coating of CS uniformly on CC.

The effect of immobilized GOx on different CS-modified CCs of Na®/CS/CC and TPP/CS/CC was investigated as shown in Fig. 3(d). The FTIR spectrum of GOx shows the peaks of the O-H broad band at 3294 cm^{-1}, C═O (Amide I) at 1639 cm^{-1}, N-H (Amide II) at 1537 cm^{-1}, and C-O-C stretching at 1018 cm^{-1}. The FTIR spectra of GOx [Na®/CS/CC] and GOx [TPP/CS/CC] show that the typical peak of amide I (C═O) stretching vibrations of native GOx observed at 1651 and 1660 cm^{-1} [56,57] and the broad band of NH_2-OH groups at 3434 cm^{-1} and 3527 cm^{-1}, respectively, confirming the immobilization of GOx into Na®/CS/CC and TPP/CS/CC. However, the intensities of GOx peaks in GOx [TPP/CS/CC] are stronger than those in GOx [Na®/CS/CC], suggesting a higher loading of GOx in GOx [TPP/CS/CC]. Such a result is also consistent with the SEM image, as shown in Fig. 2(e), presenting the higher amount of GOx distributed on TPP/CS/CC.

3.3. The electron transfer ability of various anodic electrodes

The result of CV in Fig. 4 shows that the intensities of redox current peaks at the electrolyte using 0.1 M glucose are higher than those without glucose. This fact confirms that the immobilization of GOx on both TPP/CS and Na®/CS can be performed with glucose oxidation reaction (GOR) at the oxidation potential peak about −0.4 V [11,17,58–60]. This result is also consistent with the CV analysis of CC with glucose, as shown in Fig. S2, indicating that glucose oxidation cannot occur on CC without GOx.

The result of CV using various electrodes of GOx, GOx/CS, GOx/TPP/CS, and GOx/Na®/CS on GCE is shown in Fig. 5. It can be found that the redox current peak of GOx/CS is slightly smaller than that of GOx, indicating that the catalytic activity of GOx would potentially be affected in the presence of CS due to its poor conductivity [21,57,61–63]. However, while comparing GOx/CS, GOx/TPP/CS, and GOx/Na®/CS, it is known that the electron transfer process during the glucose oxidation can be tuned by the additive within the support materials in order to reach an optimization of GOx immobilized on the electrode. Accordingly, the result of Fig. 5 indicates the sample of GOx/TPP/CS has a higher oxidation current peaks of 129.2 μA than that of GOx/Na®/CS (103.8 μA), confirming that TPP/CS-modified sample is beneficial for the immobilization sites of the glucose oxidase (GOx) and thereby facilitating more electron transfer in glucose oxidation reaction due to the formation of the open porous structure on CS-modified CC, as observed in the SEM image of Fig. 2(e).

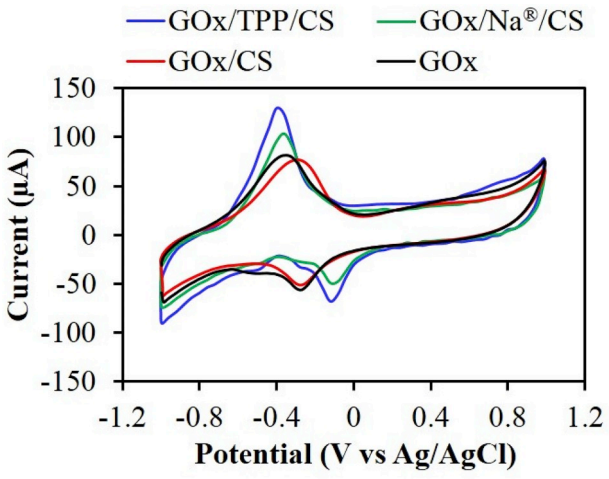

Fig. 5. CV of GOx, GOx/Cs, GOx/Na®/CS and GOx/TPP/CS on GCE in phosphate buffer saline (PBS, pH = 7) with 0.1 M $C_6H_{12}O_6$ at 100 mV s^{-1}.

3.4. The performance of enzymatic biofuel cell using various anodic electrodes

The performance of EBC using different anodic electrodes of GOx [Na®/CS/CC] and GOx [TPP/CS/CC] was evaluated as shown in Fig. 6 (a). It can be found that the typical EBC using GOx [TPP/CS/CC] has the maximum area power density of 1.471 mWcm^{-2} at 0.46 V, higher than that using GOx [Na®/CS/CC] (0.961 mWcm^{-2} at 0.42 V). This result can be attributed to the preferred open porous structure of TPP/CS/CC for the immobilization of GOx, leading to the higher loading of GOx on TPP/CS/CC, as observed in Fig. 2(e), and thereby increasing the capability of electron transfer, as revealed in Fig. 5.

A comparison study of the typical EBC and self-pumping EBC using the same anodic electrode of GOx [TPP/CS/CC] was investigated. The

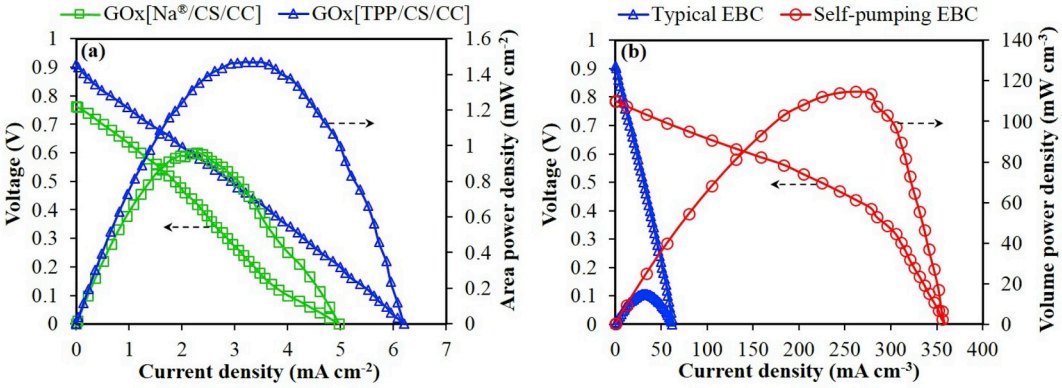

Fig. 6. (a) The polarization curves of the typical EBCs using different anodic electrodes of GOx [Na®/CS/CC]and GOx [TPP/CS/CC] operated under the test condition of the anode side using 0.1 M glucose solution at the flow rate of 0.264 mL s^{-1} and the cathode side using 0.1 M $K_3Fe(CN)_6$ solution at the flow rate of 0.274 mL s^{-1}; (b) a device performance comparison of the typical EBC and self-pumping EBC using the same anodic electrode of GOx [TPP/CS/CC]. The polarization curve of self-pumping EBC operated under the test condition of the anode side using 0.1 M glucose solution (PBS, pH 7) at the flow rate of 0.499 μL s^{-1} and the cathode side using 0.1 M $K_3Fe(CN)_6$ solution (PBS, pH 7) at the flow rate of 0.764 μL s^{-1}.

Table 1
The output power density of the typical and self-pumping EBC.

	Voltage (V)	Max. Area Power density ($mWcm^{-2}$)	Max. Volume Power density ($mWcm^{-3}$)	Note
Typical EBC	0.46	1.471 ± 0.015	14.71 ± 0.015	TPP/CS
	0.42	0.961 ± 0.022	9.61 ± 0.022	Na®/CS
Self-pumping EBC	0.44	0.549 ± 0.016	114.52 ± 0.016	TPP/CS
	0.42	0.488 ± 0.019	101.80 ± 0.019	Na®/CS

polarization curve of the self-pumping EBC (typical EBC) was conducted under the test condition of the anode side using 0.1 M glucose solution at the flow rate of 0.499 μL s^{-1} (0.264 mLs^{-1}) and the cathode side using 0.1 M $K_3Fe(CN)_6$ solution at the flow rate of 0.764 μL s^{-1} (0.274 mLs^{-1}). Table 1 indicates the summary of the output power density of the typical EBC and self-pumping EBC. The observation of maximum area power density of typical EBC (1.471 $mWcm^{-2}$ at 0.46 V) higher than self-pumping EBC (0.549 $mWcm^{-2}$ at 0.44 V), as shown in Fig. S3, can be attributed to the higher flow rate of the fuel, leading to the increase of the oxidation-reduction reaction and thereby raising the output power. However, Fig. 6(b) shows that the self-pumping EBC has a maximum volume power density of 114.52 $mWcm^{-3}$, higher than the typical EBC (14.71 $mWcm^{-3}$), making it promising for the lightweight and portable applications. The reported performance of EBCs using glucose as fuel is summarized in Table 2. It can be seen that our typical and self-pumping EBCs using GOx [TPP/CS/CC] exhibit a comparable cell performance, as compared with the previously reported results in EBCs, suggesting that a desired immobilization of GOx on CS-modified CC can be achieved via our developed facile and low-cost route.

To evaluate the stability of the chitosan-modified CC, the time-dependent performance of the self-pumping EBC using GOx [TPP/CS/CC] and GOx [Na®/CS/CC] electrodes operated at 0 h, 24 h, 72 h, 120 h, and 240 h was investigated as shown in Fig. 7. The result indicates that the area power density of self-pumping EBC using GOx [TPP/CS/CC] is

Table 2
Reported performance of EBCs using glucose as fuel.

EBCs		Fuel (mM)	Power density ($mW\ cm^{-2}$)	Driven Force/Flow rate	Ref.
Anode	Cathode				
GOx/PPy/HQS	Lac/PPy/ABTS	10	0.042	N/A	[64]
GOx/SWNT/pSi	Lac/SWNT/pSi	4	0.0014	N/A	[65]
GOx/HQS/PPy	Lac/ABTS/PPy	10	0.027	N/A	[66]
GOx/Osimium redox polymer/GE	Lac/Osimium redox polymer/GE	10	0.04	N/A	[67]
GOx/BZQ	Lac/ABTS	100	0.02	N/A	[68]
GOx/$Fe(CN)_6^{3-}$	Lac/ABTS	10	0.11	1.0 mL/min	[69]
GOx [GDH/NB/f- SWCNTs/GC]	Lac/MG-SWCNTs/GC	40	0.03	N/A	[70]
GOx/GCS/NCNTs/GCE	Lac/GCS/NCNTs/GCE	5	0.02	N/A	[71]
GOx/EAPC/Na®/CP	Lac/EAPC/Na®/CP	200	0.04	0.4 mL/min	[72]
GOx/SWNT/Ppy	Tyrosinase/CNP/Ppy	20	0.16	N/A	[73]
GOx/CNT	Lac/CNT	50	1.30	N/A	[26]
GOx/GO/$Co(OH)_2$/CS	Lac/GO/$Co(OH)_2$/CS	100	0.52	N/A	[74]
TPA [GOx/PEI/CNT]	Pt/C	200	0.98	60 mL/min	[17]
Pt/C	[CNT/Lac/PEI/Lac]/GA	40	0.20	100 mL/min	[16]
(GOx-GMC)/Na®	Pt/C	10	0.02	Peristaltic pump	[75]
MWCNT-COOH/Ni complex	CC	200 (sucrose)	0.41	N/A	[76]
EGDGE/PEI/MWCNT	BOx/MWCNT/Nafion	5	0.03	2.55 μL s^{-1}	[77]
GOx/Copper (II) sulfat/CNT	Lac/Copper (II) sulfat/CNT	50	0.22	N/A	[78]
Na®/GOx/PANI 1600@CNT/GCE	Na®/Lac/PANI1600 @CNT/GC	100	1.12	N/A	[79]
[(TPA/HRP/GOx)]/PEI/CNT	Pt/C	200	2.0	60 mL/min	[80]
GOx [TPP/CS/CC]	$K_3Fe(CN)_6$/CC	100	1.47	16.4 mL/min	This work
GOx [Na®/CS/CC]	$K_3Fe(CN)_6$/CC	100	0.96	16.4 mL/min	This work
GOx [TPP/CS/CC]	$K_3Fe(CN)_6$/CC	100	0.55	Self-pumping 0.499 μLs^{-1}	This work

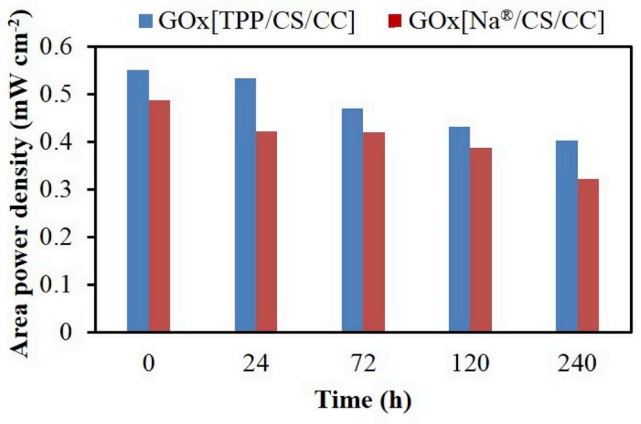

Fig. 7. Stability testing of self-pumping EBC using GOx [TPP/CS/CC] and GOx [Na®/CS/CC] as anodic electrodes operated at 0 h, 24 h, 72 h, 120 h, and 240 h at room temperature.

decreased from 97.1% (24 h) to 73% (240 h) of its initial value while that of using GOx [Na®/CS/CC] is decreased from 86.5% (24 h) to 66% (240 h) of its initial value. Such the decreasing trends can be mainly attributed to the effect of the GOx leaching and its degradation by hydrogen peroxide (H_2O_2) with the time [61,80,81]. Accordingly, our sample of using GOx [TPP/CS/CC] exhibits a better stability than that of using GOx [Na®/CS/CC] during the operation, indicating that TPP/CS/CC can provide the strong immobilized sites to avoid the GOx leaching. The surface image of the GOx [TPP/CS/CC] electrode after 240 h was also investigated by SEM, as shown in Fig. S4, presenting that only a minor amount of GOx/TPP/CS layer is peeled off from the CC. This fact can imply that the observation of the initial decrease in the stability is mainly related to the leaching and degradation of the GOx instead of the detachment of GOx/TPP/CS from CC. However, both of our samples seemingly show a relatively rapid decay of cell performance, suggesting that the slow flow rate during the self-pumping operation could retard the removal of hydrogen peroxide (H_2O_2), resulting in an enhanced degradation of GOx. Such a result is consistent with the reference reporting the importance of H_2O_2 removal for the better stability [80,82–84].

4. Conclusions

We have successfully demonstrated a facile and low-cost route to achieve a desired immobilization of the glucose oxidase on a robust, flexible conducive carbon cloth. It is found that the immobilization of the enzyme is strongly affected by the surface property of CS-modified CC, leading to the different amount of the enzyme distributed on the anodic electrode and thereby affecting the power density. A desirable distribution of the immobilized enzyme on the anodic electrode can be obtained by using the CS-modified carbon cloth of TPP/CS/CC, leading to a 53% improvement of power density as compared with that of Na®/CS/CC. Such an improvement can be ascribed to the cross-link of CS with TPP to form an open porous structure on CC, resulting in the increase of the immobilized glucose oxidase and thereby facilitating more electron transfer in glucose oxidation reaction. The self-pumping EBC using the anodic electrode of TPP/CS/CC exhibits an efficient surface and volume power density of 0.549 $mWcm^{-2}$ and 114.52 $mWcm^{-3}$, respectively, demonstrating the promise for the lightweight and portable applications.

Conflicts of interest

The authors declare no conflict of interest.

Acknowledgements

This work is funded by the Ministry of Science and Technology, Taiwan under the grant of MOST-106-2221-E-005-074 and MOST-105-2923-E-005-001-MY3 as well as supported in part by the Ministry of Education, Taiwan, R.O.C. under the Higher Education Sprout Project.

Appendix A. Supplementary data

Supplementary data to this article can be found online at https://doi.org/10.1016/j.jpowsour.2019.05.001.

References

[1] C. Lamy, A. Lima, V. LeRhun, F. Delime, C. Coutanceau, J.-M. Léger, J. Power Sources 105 (2002) 283–296.
[2] K. Kano, Electrochemistry 71 (2003) 86–99.
[3] I. Ivanov, T. Vidaković-Koch, K. Sundmacher, Energies 3 (2010) 803–846.
[4] M. Rasmussen, S. Abdellaoui, S.D. Minteer, Biosens. Bioelectron. 76 (2016) 91–102.
[5] Z. Ghassemi, G. Slaughter, Membranes 7 (2017) 1–12.
[6] C. Santoro, C. Arbizzani, B. Erable, I. Ieropoulos, J. Power Sources 356 (2017) 225–244.
[7] X. Huang, L. Zhang, Z. Zhang, S. Guo, H. Shang, Y. Li, J. Liu, Biosens. Bioelectron. 124–125 (2019) 40–52.
[8] I. Jeerapan, J.R. Sempionatto, J.-M. You, J. Wang, Biosens. Bioelectron. 122 (2018) 284–289.
[9] A. Vaze, N. Hussain, C. Tang, D. Leech, J. Rusling, Electrochem. Commun. 11 (2009) 2004–2007.
[10] T. Tamer, A. Omer, M. Hassan, 7 (2016) 385-392.
[11] K.H. Hyun, S.W. Han, W.-G. Koh, Y. Kwon, J. Power Sources 286 (2015) 197–203.
[12] Y. Ogawa, Y. Takai, Y. Kato, H. Kai, T. Miyake, M. Nishizawa, Biosens. Bioelectron. 74 (2015) 947–952.
[13] T. Tamaki, T. Ito, T. Yamaguchi, J. Phys. Chem. B 111 (2007) 10312–10319.
[14] P.N. Barlett, J.M. Cooper, J. Electroanal. Chem. 362 (1993) 1–12.
[15] X. Wang, K.-X. Zhu, H.-M. Zhou, Int. j. molecular sciences 12 (2011) 3042–3054.
[16] M. Christwardana, Enzym. Microb. Technol. 106 (2017) 1–10.
[17] Y. Chung, Y. Ahn, M. Christwardana, H. Kim, Y. Kwon, Nanoscale 8 (2016) 9201–9210.
[18] J. Kim, J.W. Grate, Nano Lett. 3 (2003) 1219–1222.
[19] J. Zdarta, A. Meyer, T. Jesionowski, M. Pinelo, Catalysts 8 (2018) 1–27.
[20] B. Krajewska, Enzym. Microb. Technol. 35 (2004) 126–139.
[21] H. Susanto, A.M. Samsudin, N. Rokhati, I.N. Widiasa, Enzym. Microb. Technol. 52 (2013) 386–392.
[22] S. El Ichi, A. Zebda, A. Laaroussi, N. Reverdy-Bruas, D. Chaussy, M. Naceur Belgacem, P. Cinquin, D.K. Martin, Chem. Commun. 50 (2014) 14535–14538.
[23] S.W. Buckner, P.A. Jelliss, A. Nukic, E.R. Zalocusky, J. Schumacher, Bioelectrochemistry 78 (2010) 130–134.
[24] Y. Huang, X. Qin, Z. Li, Y. Fu, C. Qin, F. Wu, Z. Su, M. Ma, Q. Xie, S. Yao, J. Hu, Biosens. Bioelectron. 31 (2012) 357–362.
[25] T. Miyake, S. Yoshino, T. Yamada, K. Hata, M. Nishizawa, J. Am. Chem. Soc. 133 (2011) 5129–5134.
[26] A. Zebda, C. Gondran, A. Le Goff, M. Holzinger, P. Cinquin, S. Cosnier, Nat. Commun. 2 (2011) 1–6.
[27] D.R. Bhumkar, V.B. Pokharkar, AAPS PharmSciTech 7 (2006). E50-E50.
[28] T.I. Nasution, R. Asrosa, I. Nainggolan, M. Balyan, R. Indah, A. Wahyudi, IOP Conf. Ser. Mater. Sci. Eng. 309 (2018) 012083.
[29] S. Kucukkolbasi, Z.O. Erdoğan, J. Barek, M. Sahin, N. Kocak, Int. J. Electrochemical Science 8 (2013) 2164–2181.
[30] S. El Ichi, M.N. Marzouki, H. Korri-Youssoufi, Biosens. Bioelectron. 24 (2009) 3084–3090.
[31] H. Jonassen, A.-L. Kjøniksen, M. Hiorth, Biomacromolecules 13 (2012) 3747–3756.
[32] M. Gierszewska, J. Ostrowska-Czubenko, Progress on Chemistry and Application of Chitin and its Derivatives 21 (2016) 55–62.
[33] J. Berger, M. Reist, J.M. Mayer, O. Felt, N.A. Peppas, R. Gurny, Eur. J. Pharm. Biopharm. 57 (2004) 19–34.
[34] P. Li, Y.-N. Dai, J.-P. Zhang, A.-Q. Wang, Q. Wei, Int. J. Biomed. Sci. : IJBS 4 (2008) 221–228.
[35] M.M. Hasani-Sadrabadi, E. Dashtimoghadam, F.S. Majedi, S. Wu, A. Bertsch, H. Moaddel, P. Renaud, RSC Adv. 3 (2013) 7337–7346.
[36] S. Cosnier, A. Le Goff, M. Holzinger, Electrochem. Commun. 38 (2014) 19–23.
[37] R. Jayakumar, M. Prabaharan, S.V. Nair, H. Tamura, Biotechnol. Adv. 28 (2010) 142–150.
[38] S. T Koev, P. H Dykstra, X. Luo, G. Rubloff, W. E Bentley, G. F Payne, R. Ghodssi, Lab Chip 10 (2010) 3026–3042.
[39] Y. Yang, Y.C. Liang, International Conference on Power Engineering vol. 2007, Energy and Electrical Drives, 2007, pp. 365–370.
[40] C.C. Lai, C.K. Chung, Microsyst. Technol. 19 (2013) 379–386.
[41] Q. Lai, G.-P. Yin, Z.B. Wang, Int. J. Energy Res. 33 (2009) 719–727.
[42] K.S. Patel, M.B. Patel, Int. J. Pharmaceut. Investig. 4 (2014) 32–37.
[43] Y.-F. Tsai, C.-J. Shieh, H. Yang, Microsyst. Technol. 23 (2015) 3927–3935.

[44] S. Vimal, S. Abdul Majeed, G. Taju, K.S.N. Nambi, N. Sundar Raj, N. Madan, M. A. Farook, T. Rajkumar, D. Gopinath, A.S. Sahul Hameed, Acta Trop. 128 (2013) 486–493.
[45] S. Hassani, A. Laouini, H. Fessi, C. Charcosset, Colloid. Surf. Physicochem. Eng. Asp. 482 (2015) 34–43.
[46] M.D.L. Kabir, H. Jin Kim, S.J. Choi, J. Nanosci. Nanotechnol. 17 (2017) 8128–8131.
[47] M.N. Gupta, M. Kaloti, M. Kapoor, K. Solanki, Artificial cells, blood substitutes, Biotechnology 39 (2011) 98–109.
[48] R. Ahmad, M. Sardar, Biochem. Anal. Biochem. 4 (2015) 1–8.
[49] A.A. Magda, M.A.-E. Ali, J. Nanomed. Nanotechnol. 6 (2015) 1–9.
[50] S. Hussain, P. Jha, A. Chouksey, R. Raman, S.s. Islam, T. Islam, P.K. Choudhary, Harsh, J. Mod. Phys. 2 (2011) 538–543.
[51] U. Sen, O. Acar, S.U. Celik, A. Bozkurt, A. Ata, T. Tokumasu, A. Miyamoto, J. Polym. Res. 20 (2013) 217.
[52] H.J. Kim, K. Talukdar, M.D.L. Kabir, S.-J. Choi, J. Nanosci. Nanotechnol. 18 (2018) 5692–5696.
[53] S. Rahmah Mokhtaruddin, A.B. Mohamad, K.S. Loh, A. Kadhum, Malaysian J. Anal. Sci. 20 (2016) 670–677.
[54] A.F. Martins, D.M. de Oliveira, A.G.B. Pereira, A.F. Rubira, E.C. Muniz, Int. J. Biol. Macromol. 51 (2012) 1127–1133.
[55] F.L. Mi, S.S. Shyu, S.T. Lee, T.B. Wong, J. Polym. Sci. B Polym. Phys. 37 (1999) 1551–1564.
[56] M. Baghayeri, RSC Adv. 5 (2015) 18267–18274.
[57] X. Wang, K.-X. Zhu, H.-M. Zhou, Int. J. Mol. Sci. 12 (2011) 3042–3054.
[58] J. Zhang, X. Yu, W. Guo, J. Qiu, X. Mou, A. Li, H. Liu, Nanoscale 8 (2016) 9382–9389.
[59] X. Zhang, D. Liu, L. Li, T. You, Sci. Rep. 5 (2015), 9885-9885.
[60] M. Christwardana, D. Frattini, Chemosensors 6 (2018) 1–12.
[61] L. Fung Ang, Y. Por, M. Yam, PLoS One 10 (2015) 1–17.
[62] L.F. Ang, L.Y. Por, M.F. Yam, PLoS One 8 (2013) 1–13.
[63] G. Ozyilmaz, A. Ozyilmaz, H. Rağibe, Akyürekoğlu, Natural and Engineering Sciences 2 (2017) 123–134.
[64] A. Habrioux, G. Merle, K. Servat, K.B. Kokoh, C. Innocent, M. Cretin, S. Tingry, J. Electroanal. Chem. 622 (2008) 97–102.
[65] S.C. Wang, F. Yang, M. Silva, A. Zarow, Y. Wang, Z. Iqbal, Electrochem. Commun. 11 (2009) 34–37.
[66] L. Brunel, J. Denele, K. Servat, K.B. Kokoh, C. Jolivalt, C. Innocent, M. Cretin, M. Rolland, S. Tingry, Electrochem. Commun. 9 (2007) 331–336.
[67] F. Barrière, P. Kavanagh, D. Leech, Electrochim. Acta 51 (2006) 5187–5192.
[68] P.-C. Nien, J.-Y. Wang, P.-Y. Chen, L.-C. Chen, K.-C. Ho, Bioresour. Technol. 101 (2010) 5480–5486.
[69] A. Zebda, L. Renaud, M. Cretin, F. Pichot, C. Innocent, R. Ferrigno, S. Tingry, Electrochem. Commun. 11 (2009) 592–595.
[70] F.S. Saleh, L. Mao, T. Ohsaka, Sensor. Actuator. B Chem. 152 (2011) 130–135.
[71] W. Wei, P. Li, Y. Li, X. Cao, S. Liu, Electrochem. Commun. 22 (2012) 181–184.
[72] R.E. Kim, S.-G. Hong, S. Ha, J. Kim, Enzym. Microb. Technol. 66 (2014) 35–41.
[73] K. Min, J. Heon Ryu, Y. Je Yoo, Biotechnol. Bioproc. Eng. 15 (2010) 371–375.
[74] H. Uk Lee, H. Young Yoo, T. Lkhagvasuren, Y. Seok Song, C. Park, J. Kim, S. Wook Kim, Biosens. Bioelectron. 42 (2013) 342–348.
[75] T. Garcia-Perez, S.-G. Hong, J. Kim, S. Ha, Enzym. Microb. Technol. 90 (2016) 26–34.
[76] Y. Zhang, M.A. Arugula, S.T. Williams, S.D. Minteer, A.L. Simonian, J. Electrochem. Soc. 163 (2016) F449–F454.
[77] L. del Torno-de Román, M. Navarro, G. Hughes, J.P. Esquivel, R.D. Milton, S. D. Minteer, N. Sabaté, Electrochim. Acta 282 (2018) 336–342.
[78] M. Chung, T.L. Nguyen, T.Q.N. Tran, H.H. Yoon, I.T. Kim, M.I. Kim, Appl. Surf. Sci. 429 (2018) 203–209.
[79] Z. Kang, K. Jiao, J. Cheng, R. Peng, S. Jiao, Z. Hu, Biosens. Bioelectron. 101 (2018) 60–65.
[80] Y. Chung, D.C. Tannia, Y. Kwon, Chem. Eng. J. 334 (2018) 1085–1092.
[81] J. Harris, C. Reyes, G. P Lopez, J. Diabet. Sci. Technol. 7 (2013) 1030–1038.
[82] K. Elouarzaki, M. Bourourou, M. Holzinger, A. Le Goff, R. Marks, S. Cosnier, Energy Environ. Sci. 8 (2015) 2069–2074.
[83] V. Krikstolaityte, Y. Oztekin, J. Kuliesius, A. Ramanaviciene, Z. Yazicigil, M. Ersoz, A. Okumus, A. Kausaite-Minkstimiene, Z. Kılıç, A. Solak, A. Makaraviciute, A. Ramanavicius, Electroanalysis 25 (2013) 2677–2683.
[84] W. Jia, C. Jin, W. Xia, M. Muhler, W. Schuhmann, L. Stoica, Chemistry 18 (2012) 2783–2786.